Electronic Supplementary Material (ESI) for Journal of Materials Chemistry C.

Pressure-mediated structural phase transitions and ultrawide indirect-direct bandgaps in novel rare-earth oxyhalides

Wei Li,[a] Naihua Miao,*[ab] Jian Zhou,[a] and Zhimei Sun*[ab]

Computational details and results for structural, mechanical, electronic and optical properties. SmSI- and YOF-types structures.

1 Mechanical properties of bulk crystals.

Elastic stability criteria[1] :

ScOX:

$$C_{11} > 0, C_{11}C_{12} > C_{12}^2,$$
$$C_{11}C_{12}C_{13} + 2C_{12}C_{13}C_{23} - C_{11}C_{23}^2 - C_{23}C_{13}^2 - C_{33}C_{12}^2 > 0,$$
$$C_{44} > 0, C_{55} > 0, C_{66} > 0.$$

R-YOX:

$$C_{11} > |C_{12}|, C_{44} > 0,$$
$$2C_{13}^2 < C_{33}(C_{11} + C_{12}),$$
$$C_{14}^2 < C_{44}C_{66}.$$

P-YOX:

$$C_{11} > |C_{12}|, C_{44} > 0,$$
$$2C_{13}^2 < C_{33}(C_{11} + C_{12}),$$
$$C_{66} > 0.$$

Three of the most widely used methods to estimate bulk modulus are propose by Voigt[2], Reuss[3] and Hill[4]. Voigt defined $B_V = [(C_{11} + C_{22} + C_{33}) + 2(C_{12} + C_{23} + C_{31})]$, Reuss defined $1/B_R = [(S_{11} + S_{22} + S_{33}) + 2(S_{12} + S_{23} + S_{31})]$. B_V and B_R are rigorous upper and lower bounds respectively. Hill defined $B_{VRH} = (B_V + B_R)/2$ as better approximation to the actual elastic behaviour.

2 Calculation of carrier mobility.

The carrier mobility is based on deformation potential theory[5] and estimated by the following expression[6,7]

$$\mu_{2D} = \frac{2e\hbar^3 C}{3k_B T\,|m^*|^2 E_l^2}$$

where $\hbar$ is reduced Planck constant; e is the elementary charge; k_B is Boltzman constant; T is temperature at 300 K; $m^* = \hbar^2/[\partial^2\varepsilon(\vec{k})/\partial\vec{k}^2]$ is the charge effective mass; $E_1 = \Delta V/(\Delta l/l_0)$ represents the deformation potential coefficient, where ΔV is the shift of the band edges (conduction band minimum for electrons and valence band maximum for holes) under strain with deformation rate of $\Delta l/l_0$; C is the elastic modulus fitted by $C^{2D} = \left(\partial^2 E/\partial\delta^2\right)/S_0$, where E is the total energy, δ is the applied strain, and S_0 is the area of the optimized cell. The relaxation time of the carrier is estimated by $\tau = \mu m^*/e$.

3 Calculation of absorption coefficient.

The theoretical optical properties are based on band structure and electric dipole approximation method, and described by the dielectric function $\varepsilon(\omega) = \varepsilon^{(1)}(\omega) + i\varepsilon^{(2)}(\omega)$, where $\varepsilon^{(2)}$ is the imaginary part of relative dielectric constant determined by a summation over empty states:

$$\varepsilon_{\alpha\beta}^{(2)}(\omega) = \frac{4\pi^2 e^2}{\Omega}\lim_{q\to 0}\frac{1}{q^2}\sum_{c,v,k} 2\omega_k \delta\left(\varepsilon_{ck}\varepsilon_{vk-\omega}\right) \times \left\langle u_{ck+e_\alpha q}\middle|u_{vk}\right\rangle \left\langle u_{vk}\middle|u_{vk}u_{ck+e_\beta q}\right\rangle$$

and $\varepsilon^{(1)}$ is the real part of relative dielectric constant, defined by the usual Kramers-Kronig transformation:[8]

$$\varepsilon_{\alpha\beta}^{(1)}(\omega) = 1 + \frac{2}{\pi}P\int_0^\infty \frac{\varepsilon_{\alpha\beta}^{(2)}(\omega')\,\omega'}{\omega'^2 - \omega^2 + i\eta}d\omega'$$

[0a] School of Materials Science and Engineering, Beihang University, Beijing, 100191, China. nhmiao@buaa.edu.cn; zmsun@buaa.edu.cn
[0b] Center for Integrated Computational Materials Engineering, International Research Institute for Multidisciplinary Science, Beihang University, Beijing, 100191, China.

The absorption coefficient is assessed by $\alpha(w) = \sqrt{2}\omega\left[\sqrt{\varepsilon_1^2(\omega)+\varepsilon_1^2(\omega)} - \varepsilon_1(w)\right]^{1/2}$ [9]. For 2D materials, dielectric function depends on the thickness of the vacuum layer when the low-dimensional systems are simulated with large interlayer distance L. To avoid this problem, we adopted optical conductivity to to represent the optical properties. According to Maxwell equation,the 3D optical conductivity can be expressed as [10]

$$\varepsilon(\omega) = 1 + \frac{i}{\varepsilon_0\omega}\sigma(\omega)$$

The in-plane 2D conductivity is directly related to that of the the 3D conductivity of the superlattice we used [10]:

$$\sigma_{2D} = L\sigma_{SL}$$

The absorbance is approximated by [11]

$$A = \frac{Re\tilde{\sigma}}{|1+\tilde{\sigma}/2|^2}$$

where $\tilde{\sigma}(\omega) = \sigma_{2D}(\omega)/\varepsilon_0 c$.

Table S1 Experimental and calculated lattice parameters (a, b, c) of bulk crystals and the relative difference between experimental and calculated data. Calculated electronic bandgaps from GGA and GGA+U methods in comparison with HSE06 functional.

Materials	Lattice constant						Band gap	
	Method	a (Å)	b (Å)	c (Å)	V (Å^3)	diff. (%)	Method	Eg (eV)
ScOCl	Expt.[1]	3.465	3.955	8.178	112.072	—	HSE06	6.26
	GGA	3.446	3.954	8.123	110.659	-1.26	GGA	4.06
	GGA+U	3.665	4.234	8.178	126.900	13.23	GGA+U	6.00
ScOBr	Expt.[2]	3.551	3.954	8.700	122.146	—	HSE06	5.26
	GGA	3.532	3.948	8.643	120.517	-1.33	GGA	3.17
	GGA+U	3.733	4.220	8.703	137.104	12.25	GGA+U	5.01
R-YOCl	Expt.[3]	3.776	3.776	27.950	345.125	—	HSE06	5.97
	GGA	3.796	3.796	28.004	349.494	1.27	GGA	4.33
	GGA+U	3.909	3.909	27.968	370.170	7.26	GGA+U	4.83
R-YOBr	Expt.	—	—	—	—	—	HSE06	5.05
	GGA	3.829	3.829	29.817	378.600	—	GGA	3.68
	GGA+U	3.937	3.937	29.869	400.986	—	GGA+U	4.11
P-YOCl	Expt.[3]	3.908	3.908	6.605	100.895	—	HSE06	6.60
	GGA	3.904	3.904	6.604	100.630	-0.26	GGA	5.02
	GGA+U	4.057	4.057	6.600	108.638	7.67	GGA+U	5.10
P-YOBr	Expt.[3]	3.845	3.845	8.255	122.042	—	HSE06	5.82
	GGA	3.837	3.837	8.337	122.772	0.60	GGA	4.42
	GGA+U	3.983	3.983	8.013	127.138	4.18	GGA+U	4.46

[1] Reference[12], *[2]* Reference[13], *[3]* Reference[14]

Table S2 Stiffness tensors C_{ij} (GPa) of bulk crystals. ScOX and YOX have 9 and 6 independent elastic constants, respectively. ($C_{66} = (C_{11} - C_{12})/2$ in R-YOX.) B_V, B_R and B_{VRH} (GPa) are bulk modules based on Voigt, Reuss and Hill schemes respectively. G_{VRH} (GPa), E_{VRH} (GPa), ν_{VRH} are shear modulus, Young's modulus and Poisson ratio based on Hill schemes.

	ScOCl	ScOBr	R-YOCl	P-YOCl	R-YOBr	P-YOBr
C_{11}	153.2	142.9	122.1	157.1	116.4	141.5
C_{12}	45.9	42.9	41.2	52.0	40.0	35.2
C_{13}	12.9	14.7	14.2	63.9	14.9	18.7
C_{14}	—	——	1.9	—	1.6	—
C_{22}	139.8	131.9	—	—	—	—
C_{23}	13.9	16.4	—	—	—	—
C_{33}	28.6	36.5	37.8	91.4	42.4	32.4
C_{44}	10.3	9.9	8.6	25.9	7.8	15.8
C_{55}	13.2	13.9	—	—	—	—
C_{66}	57.9	53.8	40.5	66.6	38.2	50.2
B_V	51.9	51.0	46.8	85.0	46.1	51.2
B_R	26.3	31.9	31.7	80.3	34.1	30.2
B_{VRH}	39.0	41.4	39.2	82.6	40.1	40.7
G_{VRH}	25.7	25.2	20.3	35.2	19.2	27.3
E_{VRH}	63.1	62.8	52.0	92.4	49.7	66.9
ν_{VRH}	0.23	0.25	0.28	0.31	0.29	0.23

Table S3 Optimized bond lengths and angles of bulk YOBr crystals.

	d_{Y-Br} (Å)	d_{Y-O} (Å)	$\theta_{Br-Y-Br}$ (deg)	θ_{Br-Y-O} (deg)	θ_{O-Y-O} (deg)
R-YOBr	2.93	2.27/2.28	82	78	76/114
P-YOBr	3.18	2.23	74	75	75

Table S4 Lattice parameter (a, b) of monolayers from GGA-PBE calculations. Bandgap energy (E_g) calculated by GGA, GGA+U and HSE06 functionals. Data taken from other theoretical work are given in parentheses.

Materials	a (Å)	b (Å)	E_g (eV)		
			GGA	GGA+U	HSE06
ScOCl	3.436 (3.477)[1]	3.947 (3.980)[1]	4.12 (4.24)[1]	6.10	6.37 (6.46)[1]
ScOBr	3.527 (3.567)[1]	3.942 (3.979)[1]	3.15 (3.21)[1]	5.11	5.25 (5.24)[1]
R-YOCl	3.781 (3.814)[2]	3.781 (3.814)[2]	4.43 (4.40)[2]	5.02	6.04
R-YOBr	3.818	3.818	3.68	4.22	5.05

[1] Reference [15], *[2]* Reference [16]

Table S5 Calculated deformation-potential constant (E_1), 2d elastic modulus (C_{2d}), effective mass in the unit of free-electron mass (m^*/m_0), carrier mobility (μ) and relaxation time (τ) for electron (e) and hole (h) along the x and y or zigzag and armchair directions for of monolayers at 300 K.

Material	Direction	Carrier type	E_1 (eV)	C_{2d} (J/m^2)	m^*/m_0	μ (cm^{2}V^{-1}s^{-1})	τ (ps)
ScOCl	x	h	5.12	113.67	3.67	4.58	0.010
		e	5.16	113.67	0.63	154.64	0.055
	y	h	1.62	99.04	1.17	393.87	0.261
		e	2.85	99.04	1.33	98.43	0.074
ScOBr	x	h	0.22	112.37	2.81	4085.71	6.519
		e	5.39	112.37	0.47	249.63	0.067
	y	h	3.48	98.77	0.68	247.41	0.096
		e	3.41	98.77	1.11	97.49	0.062
R-YOCl	zigzag	h	9.67	100.58	1.57	6.19	0.006
		e	3.99	100.58	0.62	234.18	0.082
	armchair	h	10.79	97.90	17.57	0.04	0.0004
		e	3.94	97.90	0.62	233.29	0.082
R-YOBr	zigzag	h	1.64	101.81	1.56	221.97	0.196
		e	1.42	101.81	0.59	2050.67	0.688
	armchair	h	1.80	99.11	3.34	38.86	0.074
		e	1.50	99.11	0.59	1803.20	0.605

S. H. et [15] reported 2D ScOCl possesses electron effective mass of 0.78, 2.9 and hole effective mass 4.18, 1.28 through GGA method, which are comparable with our calculations.

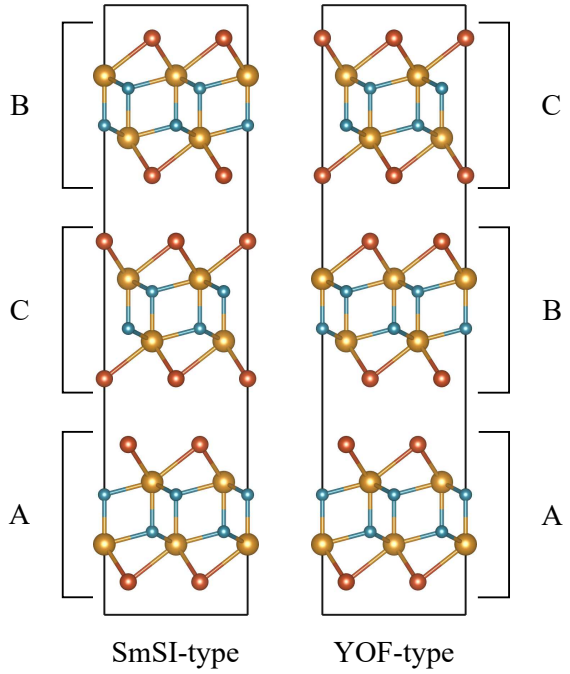

Figure S1 Projections of of the SmSI-type and YOF-type structures along (110) plane. Metal, chalcogen and halogen atoms are shown in yellow, blue and red, respectively.

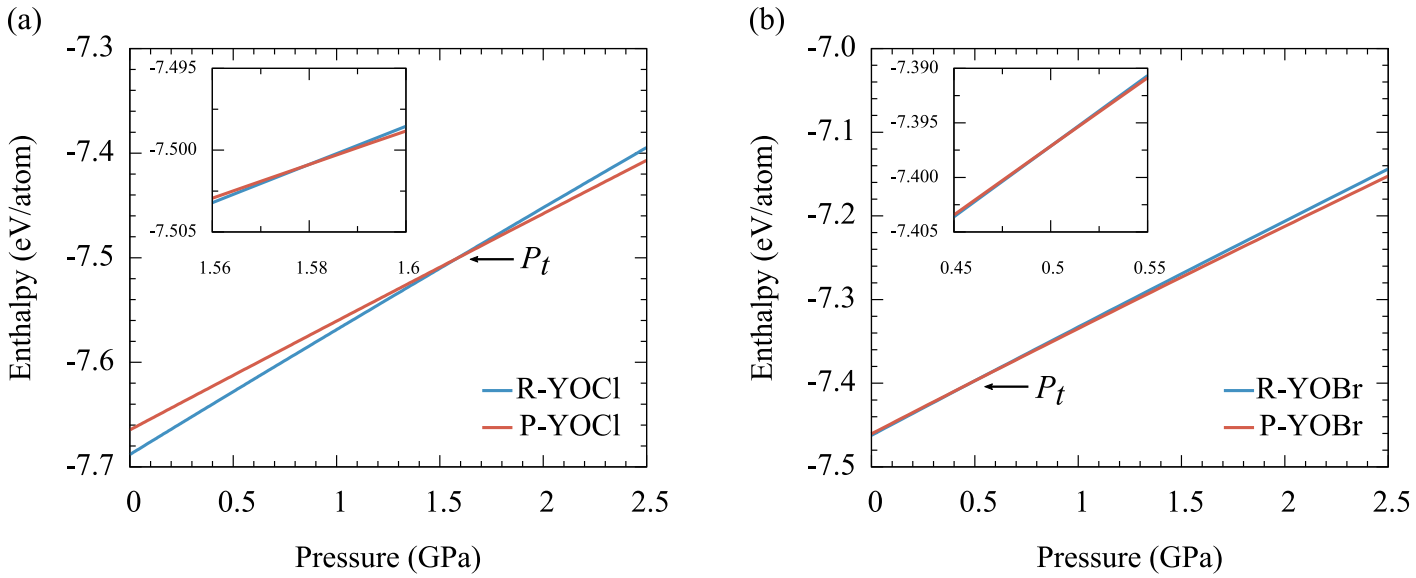

Figure S2 Enthalpy vs pressure for trigonal and tetragonal phases of (a) YOCl and (b) YOBr. The insets illustrate the curves around the transition point. Phase-transition pressures P_t are denoted by the arrows.

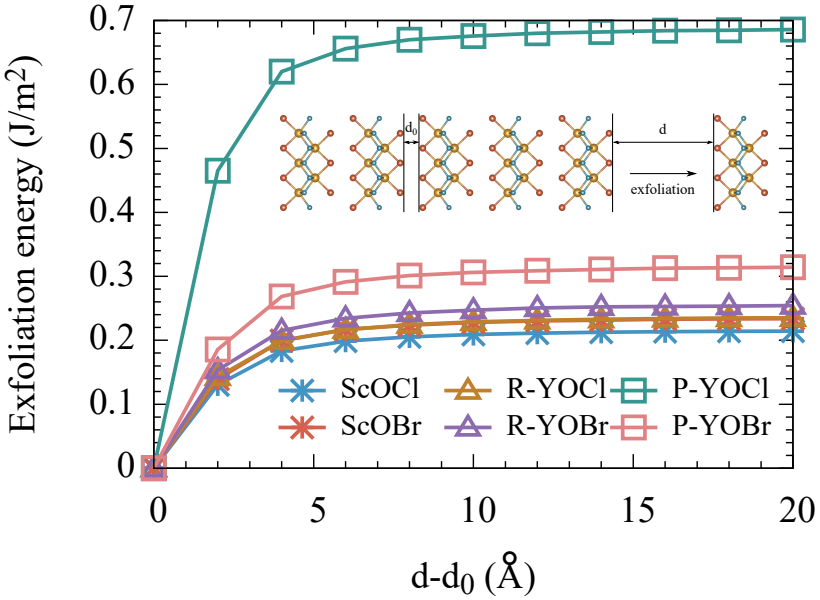

Figure S3 Exfoliation energy vs separation distance d-d_0, where d_0 is the vdw gap between immediate layers of MOX bulk crystals.

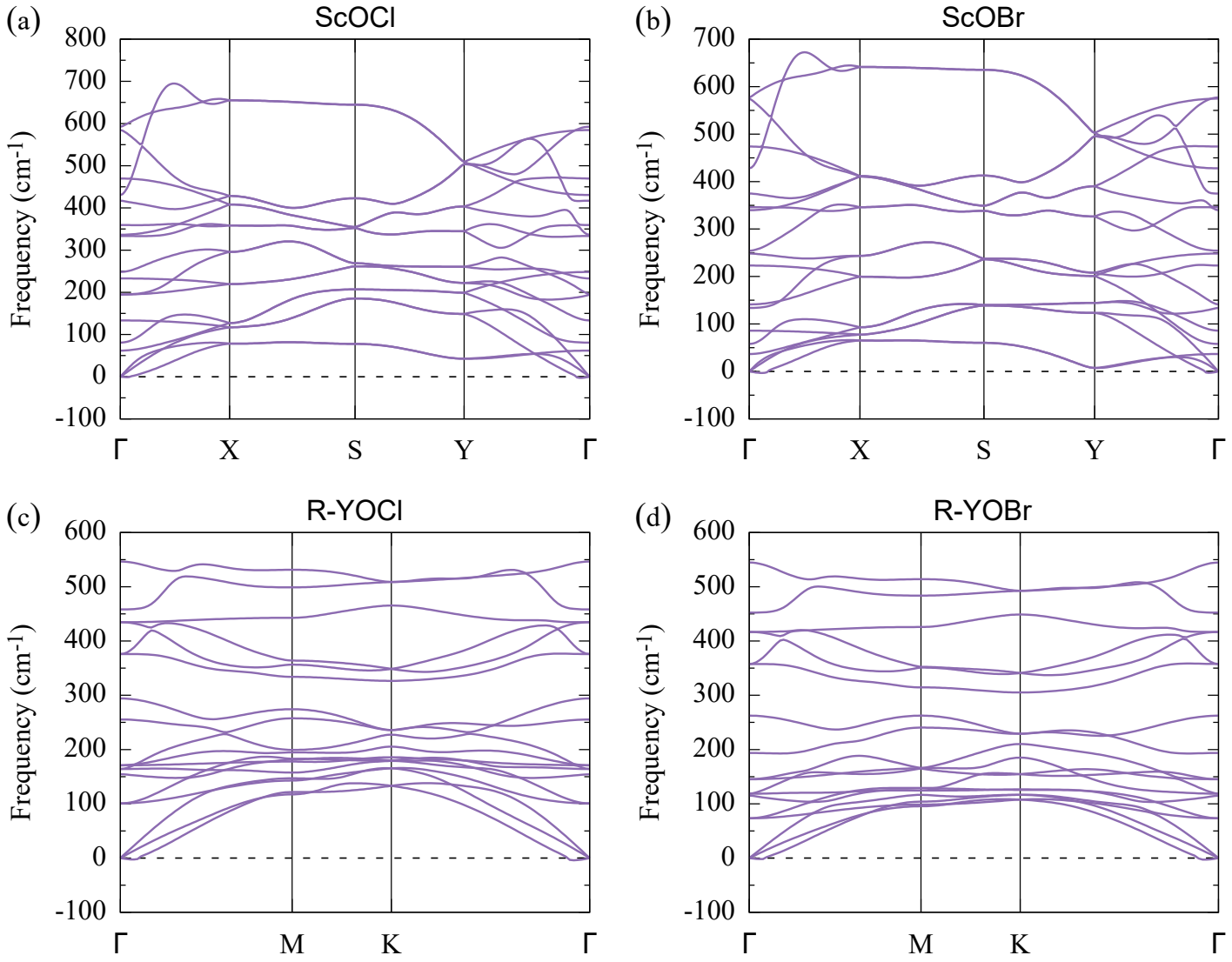

Figure S4 Phonon dispersions of MOX monolayers.

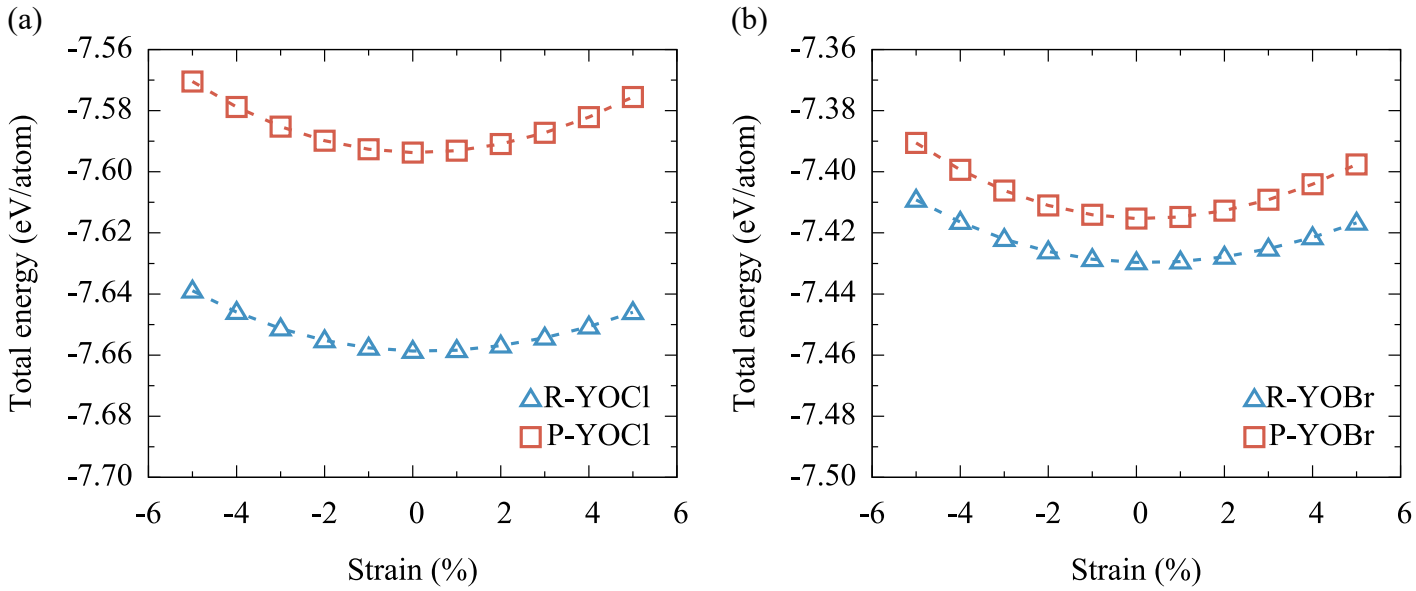

Figure S5 Total energy of the trigonal and tetragonal YOCl and YOBr monolayers under uniaxial strains.

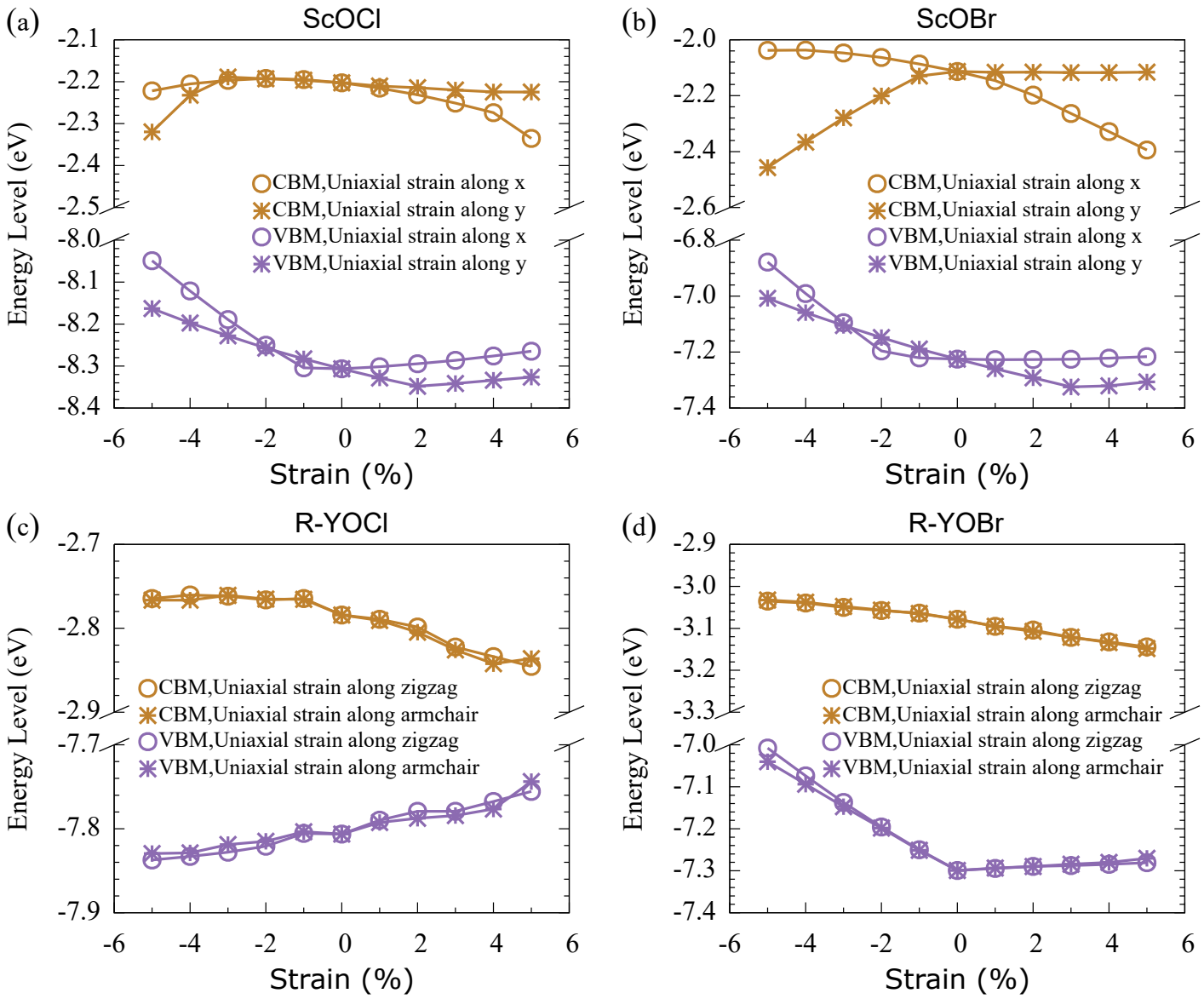

Figure S6 The conduction band minimum and valence band maximum (CBM and VBM) under strain of MOX monolayers, where the vacuum level is set to be zero.

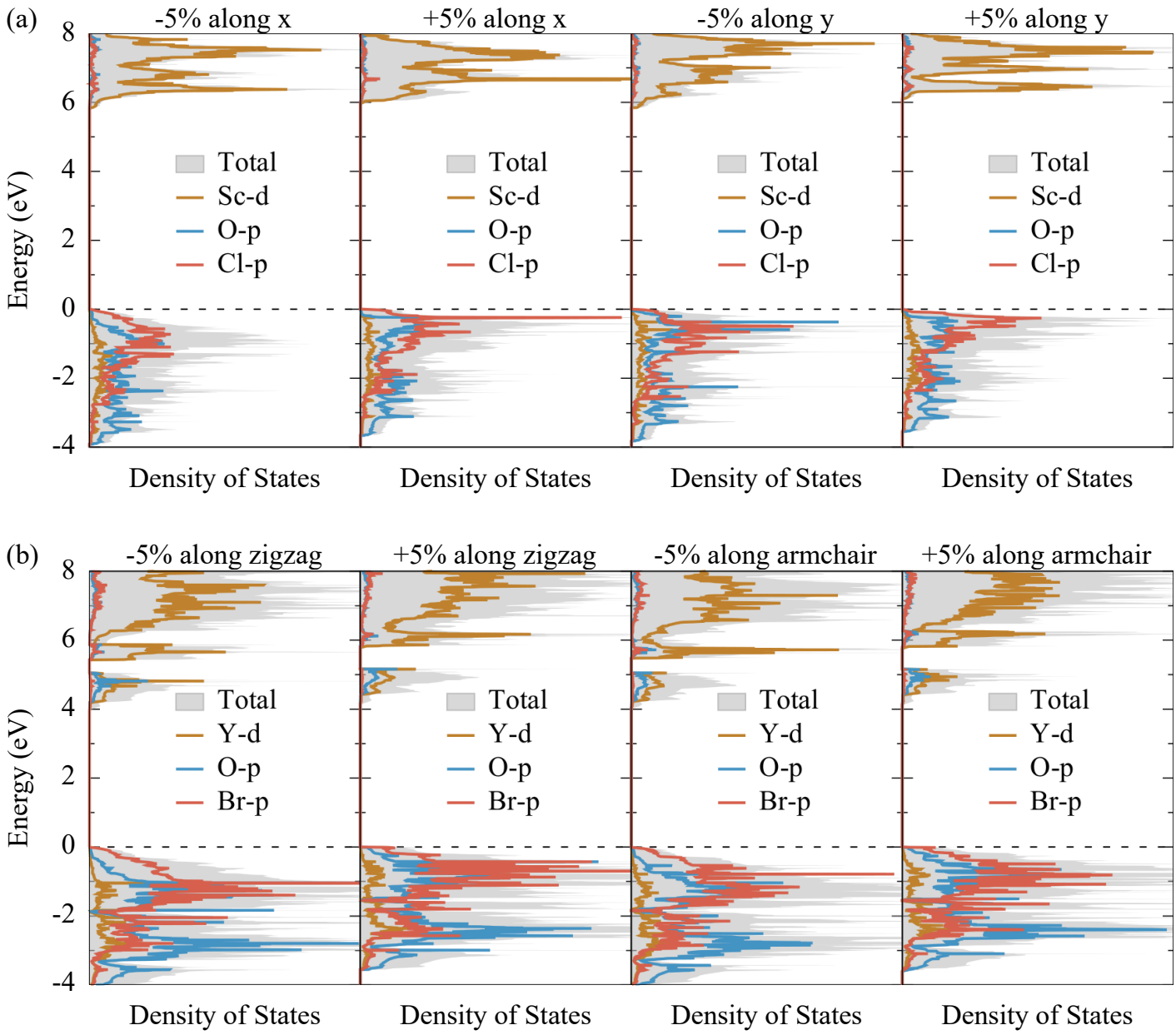

Figure S7 Calculated electronic density of states of (a) ScOCl and (b) R-YOBr monolayers under -5% and +5% uniaxial strains along different directions.

Notes and references

[1] F. Mouhat and F.-X. Coudert, *Phys. Rev. B*, 2014, **90**, 224104.

[2] W. Voigt *et al.*, *Lehrbuch der kristallphysik*, Teubner Leipzig, 1928, vol. 962.

[3] A. Reuss, *Math. Mech*, 1929, **9**, 55.

[4] R. Hill, *Proc. Phys. Soc. London, Sect. A*, 1952, **65**, 349–354.

[5] J. Bardeen and W. Shockley, *Phys. Rev.*, 1950, **80**, 72–80.

[6] J. Xi, M. Long, L. Tang, D. Wang and Z. Shuai, *Nanoscale*, 2012, **4**, 4348.

[7] J. Dai and X. C. Zeng, *Angew. Chem. Int. Ed.*, 2015, **54**, 7572–7576.

[8] M. Gajdoš, K. Hummer, G. Kresse, J. Furthmüller and F. Bechstedt, *Phys. Rev. B*, 2006, **73**, 045112.

[9] S. Saha, T. P. Sinha and A. Mookerjee, *Phys. Rev. B*, 2000, **62**, 8828–8834.

[10] L. Matthes, O. Pulci and F. Bechstedt, *New J. Phys.*, 2014, **16**, 105007.

[11] L. Matthes, O. Pulci and F. Bechstedt, *Phys. Rev. B*, 2016, **94**, 205408.

[12] E. Garcia, J. D. Corbett, J. E. Ford and W. J. Vary, *Inorg. Chem.*, 1985, **24**, 494–498.

[13] L. Jongen and G. Meyer, *Acta Crystallogr., Sect. E: Struct. Rep. Online*, 2005, **61**, i153–i154.

[14] G. Meyer and T. Staffel, *Z. Anorg. Allg. Chem.*, 1986, **532**, 31–36.

[15] S. Haastrup, M. Strange, M. Pandey, T. Deilmann, P. S. Schmidt, N. F. Hinsche, M. N. Gjerding, D. Torelli, P. M. Larsen, A. C. Riis-Jensen, J. Gath, K. W. Jacobsen, J. J. Mortensen, T. Olsen and K. S. Thygesen, *2D Mater.*, 2018, **5**, 042002.

[16] N. Mounet, M. Gibertini, P. Schwaller, D. Campi, A. Merkys, A. Marrazzo, T. Sohier, I. E. Castelli, A. Cepellotti, G. Pizzi and N. Marzari, *Nat. Nanotechnol.*, 2018, **13**, 246–252.